Modeling of Heterogeneous Electrophysiology in the Human Heart with Respect to ECG Genesis

DL Weiss[1], G Seemann[1], DUJ Keller[1], D Farina[1],
FB Sachse[2], O Dössel[1]

[1]Institute of Biomedical Engineering, Universität Karlsruhe, Karlsruhe, Germany
[2]Nora Eccles Harrison Cardiovascular Research and Training Institute, University of Utah, Salt Lake City, Utah, USA

Abstract

Heterogeneity of ion channel properties within human ventricular tissue determines the sequence of repolarization under healthy conditions. In this computational study, the impact of different extend of electrophysiological heterogeneity in both human ventricles on the ECG was investigated by a forward calculation of the cardiac electrical signals on the body surface. The gradients ranged from solely transmural, interventricular and apico-basal up to full combination of these variations. As long interventricular heterogeneities were neglected, the transmural gradient generated a positive T wave that was increased when apico-basal variations were considered. Inclusion of interventricular changes necessitated the incorporation of both transmural and apico-basal heterogeneities to reproduce the positive T wave.

1. Introduction

More than 100 years after Einthoven's first measurement of the human ECG, there are still discussions about the genesis of the T wave in the body surface ECG. The same polarity of T wave and QRS complex must be due to an altered global repolarization versus activation sequence within the tissue. This effect is mainly caused by heterogeneities within the heart influencing the intrinsic electrophysiological properties of the cardiomyocytes. Transmural, apico-basal, and interventricular heterogeneities have been observed in human ventricular tissue [1].

Transmural dispersion was shown in different ion channel properties across the human ventricular wall. The transient outward current I_{to} is significantly larger in epicardial than in endocardial cells in the human right and left ventricle (RV, LV) [2, 3, 4, 5]. Furthermore, the rate-dependent properties of I_{to} are varying transmurally in the human LV. The time course of recovery from inactivation is clearly faster in epicardial than in endocardial cells [4]. Measurements of ventricular variations of the delayed rectifier current I_{Ks} and the sodium-calcium exchanger current I_{NaCa} were only conducted on larger animals but not on human cardiomyocytes. The mean value of I_{Ks} in canine M cells was about half of endocardial cells which in turn developed 92 % of the epicardial value [6]. I_{NaCa} was large in M and epicardial but significantly smaller in endocardial canine LV myocytes [7].

Current measurements during a voltage step to +60 mV revealed that human mean epicardial I_{to} in the RV is 88 % of its value in the LV whereas endocardial differences between both ventricles were only marginal [2, 3]. Interventricular steady-state inactivation and rate of recovery of I_{to} were similar in canine [8]. Mean value of I_{Ks} in canine M cells was nearly doubled in the RV compared to the LV [8].

Concerning apico-basal variations only a few experiments were conducted in large animals. Mainly the density of I_{Ks} varied in the left epicardial layers in canine [9].

In this computational study different setups of heterogeneously distributed ion channel characteristics within both ventricles of the Visible Man dataset were investigated. Configurations ranged from homogeneity over variations in one direction up to three-dimensional heterogeneity including transmural, interventricular, and apico-basal gradients. The contribution of various distributions of heterogeneities to the corresponding ECG was investigated.

2. Methods

The properties of the human ventricular electrophysiology were characterized by the ten Tusscher model [10]. The model itself contained a transmurally heterogeneous description for the maximum conductance of I_{Ks} and for the properties of I_{to}. These heterogeneities were extended according to the described measurements. The maximum conductance g_{Ks} in the endocardium was reduced to 92 % of its epicardial value. In M cells g_{Ks} was reduced to 79 % of the original specification to obtain real-

	position	Endo	M	Epi base	Epi apex
g_{to}	LV	0.073	0.294	0.294	0.294
(nS/pF)	RV	0.073	0.258	0.258	0.258
g_{Ks}	LV	0.2254	0.049	0.245	0.49
(nS/pF)	RV	0.426	0.093	0.463	0.463
k_{NaCa}	LV	1.00	1.50	1.39	1.39
(pA/pF)	RV	1.00	1.00	1.00	1.00
APD	LV	278	317	268	237
(ms)	RV	246	309	241	241

Table 1. Transmural, interventricular, and apico-basal gradients of the maximum conductances of the currents I_{to}, I_{Ks}, and I_{NaCa} used in this study and the corresponding APDs in single cell environment. Additionally, the parameters defining the recovery from inactivation of I_{to} are heterogenously distributed in transmural direction in both ventricles [10].

istic action potential durations (APD). Additionally, a heterogeneous distribution of I_{NaCa} with largest value in M and smallest in endocardial cells was introduced. Interventricular heterogeneities were incorporated for I_{to} and I_{Ks} whereas the published specification [10] served as a characterization of the LV. Apico-basal variations were considered for the left epicardial I_{Ks} by doubling its basal compared to the apical conductivity. Table 1 summarizes the utilized parameter distributions. Values between the given anchor points were approximated using cubic splines in transmural and linear interpolation in apico-basal direction.

Every setup was pre-computed in a single cell until a steady state was reached. The virtual cells with isotropic conductivities were electrically coupled using the monodomain approach.

Both ventricles of the Visible Man dataset embedded in its torso [11] were used as underlying anatomical structure. The dataset of the ventricles was interpolated to cubic volume elements with a side length of 0.4 mm. The resulting heart model consisted of 279 x 254 x 259 volume elements whereof more than 4.4 Mio. belonged to excitable tissue. The electrical activation system was generated automatically reconstructing the activation sequence of the Purkinje system. The torso model had a grid size of 2 mm and consisted of 297 x 170 x 260 volume elements. Several organs were distinguished in their conductivities: lungs, blood, muscle, fat, etc..

The forward calculation of the Body Surface Potential Map (BSPM) was performed on a tetrahedral mesh of both heart and thoracic geometry consisting of 113839 nodes. The transmembrane voltages V_m were interpolated onto the mesh of the ventricles and the extracellular potentials

configuration	v_{peak} (mV)	t_{peak} (ms)
homo,epi	-0.688	290
homo,M	-0.598	340
iv	-0.858	292
ab	-0.298	273
tm	0.503	325
tm+iv,base	-0.531	289
tm+iv,apex	-0.208	262
(biphasic)	0.537	306
ab+iv	-0.462	267
tm+ab	0.574	301
full	0.431	301

Table 2. Impact of different configurations of heterogenously distributed ion channel characteristics on the properties of the Einthoven II lead. v_{peak} describes the voltage of and t_{peak} the time to the T wave peak.

ϕ_e on the body surface were calculated by

$$\nabla \cdot (\sigma \nabla \phi_e) = -\nabla \cdot (\sigma_i \nabla V_m)$$

with σ_i the intracellular and σ the combined intra- and extracellular conductivity tensor including unequal anisotropy ratios. ECGs were determined by computing the difference of ϕ_e. The electrode positions for the utilized Einthoven II lead generating positive T waves for healthy patients are shown in the left column of Fig. 2.

3. Results

The shape of the computed action potential (AP) was determined by the location of the cardiomyocyte and the corresponding electrophysiological characteristics. Besides the transmural properties, right ventricular and left apical APs were shortened due to their increased I_{Ks}.

To investigate the influence of electrophysiological heterogeneities on the ECG, a homogeneous parameter distribution served as reference. Configuration ***homo,epi*** was calculated with LV basal epicardial and ***homo,M*** with LV M cell electrophysiology (see Table 1) in the entire tissue. In both cases, the sequence of repolarization followed the sequence of activation and the ECG developed a negative T wave (see Fig. 1). The value of the T wave peak (v_{peak}) was marginally influenced by the utilized parameter set (see Table 2). However, the time t_{peak} to v_{peak} was clearly determined by the respective configuration.

Unless mentioned otherwise, the global electrophysiology in the subsequent heterogeneous simulations was basically taken from the basal epicardial configuration of the LV. A simulation with solely inclusion of interventricular variances was named ***iv***. Right ventricular g_{to} and g_{Ks} are set to RV epicardial values. The increased I_{Ks} in the RV resulted in its accelerated repolarization. While

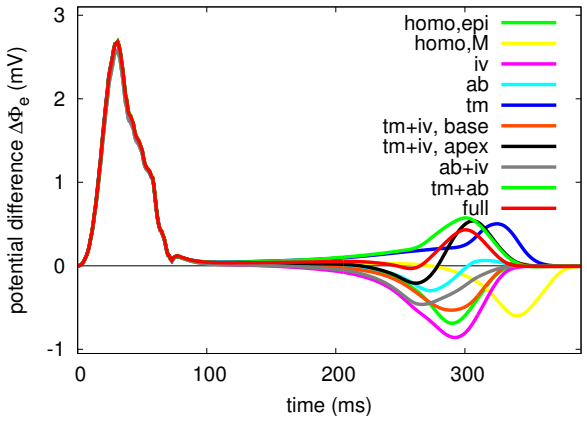

Figure 1. ECGs computed with the different heterogeneous ion channel distributions.

t_{peak} in ***iv*** was comparable to ***homo,epi***, v_{peak} was more negative than in the homogeneous configurations. The ***ab*** setup exclusively considered the reported apico-basal changes of I_{Ks} within the entire LV. The apex of the LV was the first to repolarize. As in the homogeneous setups, the repolarization started in endocardium and ended in epicardium. The corresponding T wave was negative. For the ***tm*** setup the transmural heterogeneities of the LV base were included in both ventricles. The prolonged APD in the M cells resulted in a shift of the end repolarizing zone towards M cells. The repolarization started nearly synchronously in the epicardium of RV and LV and the ECG developed a late positive T wave.

The configuration ***tm+iv,base*** combines ***tm*** and ***iv*** leading to a faster repolarization in the RV. The resulting T wave was negative. The setup ***tm+iv,apex*** is comparable however g_{Ks} in the left epicardium was set to its higher apical value. The effect was an accelerated repolarization of the left epicardium resulting in a biphasic T wave. The composition of ***ab*** and ***iv*** is described by ***ab+iv***. The shorter APs in the RV and left ventricular apex sped up the repolarization in these areas and the v_{peak} was less negative than in ***iv***. For the ***tm+ab*** configuration ***tm*** and ***ab*** were linked. The apico-basal distribution of the I_{Ks} density varied within the left epicardial myocardium. The repolarization sequence was comparable to the ***tm*** setup but faster in the LV apex. The positive T wave developed the largest amplitude of all configurations.

The final ***full*** setup combined all heterogeneities shown in Table 1. The corresponding three-dimensional distribution for g_{Ks} is visualized in the left column of Fig. 2. The resulting repolarization manifested faster in the RV and apical LV than in the LV base. The sequence of activation and repolarization for this configuration is shown in Fig. 2. The T wave resulting from this most realistic setup was positive.

4. Discussion and conclusions

The impact of different heterogeneous distributions of ion channel characteristics on the human ECG was investigated. The activation was not determined by the heterogeneity of the ionic currents. Thus, all configurations lead to the similar QRS complex. However, the repolarization sequence was mainly determined by the dispersion of the repolarizing I_{Ks} current.

The T wave was more negative the closer the repolarization started in endocardium (***homo,epi***, ***homo,M***). Inclusion of transmural heterogeneity moved the final repolarization towards M cells and the repolarization sequence started preferentially in the epicardium. The T wave for ***tm*** was positive. Earlier repolarization of the RV compared to LV reduced the maximum T wave amplitude (***tm*** vs. ***tm+iv,base***). Configuration ***iv*** developed the most negative value for v_{peak}. Incorporation of an apico-basal gradient of I_{Ks} shortened left apical APDs. Thus, the repolarization was faster in the LV apex than base. The maximum of the T wave was increased and appeared earlier (***iv*** vs. ***ab+iv*** or ***tm*** vs. ***tm+ab***). The ***full*** configuration considered all heterogeneities and the v_{peak} reducing effect of ***iv*** was suppressed by the combination of ***tm*** and ***ab***. The corresponding T wave showed realistic positive values.

A limitation of the study is the little amount of measurements concerning human ventricular heterogeneities of the electrophysiology. Measurements of human I_{Ks} distributions are missing but the existence of M cells in the human RV [2] and a shorter APD in RV compared to LV [12] was demonstrated. Thus, a transmural and interventricular distribution of I_{Ks} comparable to canine was incorporated in the parameter sets [6, 8]. However, the specification of the apico-basal gradient of I_{Ks} was inverted for the presented human setup compared to canine measurements. Bauer et. al [9] detected reduced I_{Ks} and therefore prolonged APs in the canine epicardial layers of the apex. However, lead II in canine shows pronounced negative T waves [13]. In human the T wave is positive and left apical APs are shorter than basal ones [12].

Our results are comparable with computational experiments conducted by Rudy et al. and van Oosterom [12, 14]. Both reconstructed epicardial potentials leading to positive T waves. The resulting APD increased from the right towards the left ventricle, as well as from apex towards base which is similar to the results of the ***full*** configuration.

As long as the interventricular gradient was neglected, a transmural setup in both ventricles generated a realistic positive T wave that was larger when auxiliary apico-basal changes in the LV were considered. Inclusion of interventricular variances necessitated the additional consideration of transmural as well as apico-basal heterogeneities to generate positive T waves in the body surface ECG.

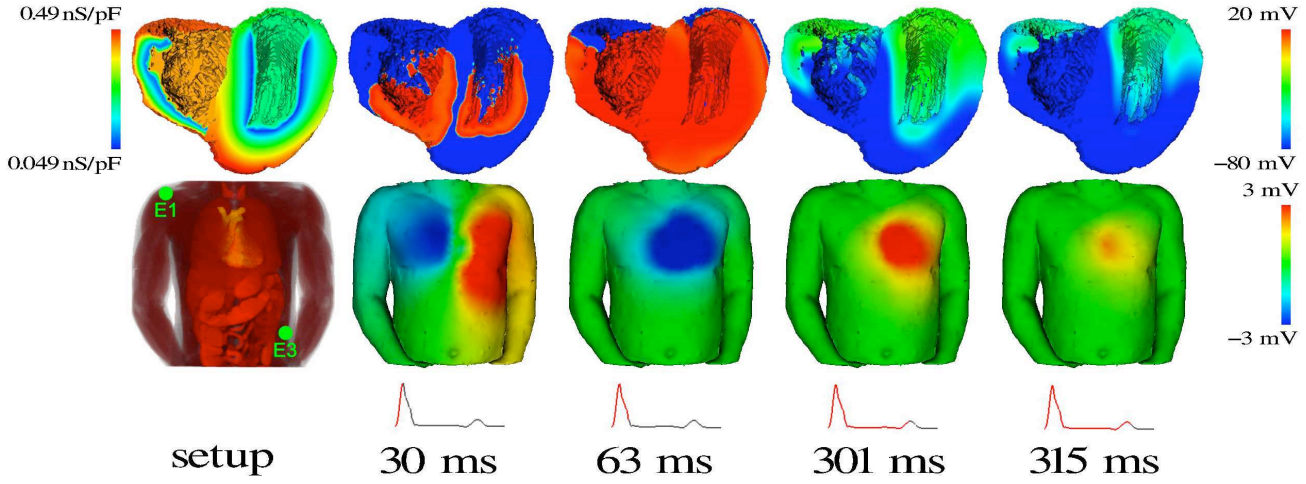

Figure 2. First column: Heterogeneous distribution of the maximum conductance g_{Ks} of the I_{Ks} current used with the ***full*** configuration (top) and interior view of the torso model with ECG lead positions (bottom). Next columns: Excitation conduction in the ventricles of the Visible Man dataset (top) with the ***full*** configuration together with the corresponding BSPM and ECG (bottom). The activation sequence started in the apical endocardium of the RV and LV and conducted first in apical and later in basal epicardial direction. After having passed the plateau phase the repolarization started at the apical epicardium and vanished in basal midmyocardium. The ventricles were cut for visualization only.

References

[1] Burton FL, Cobbe SM. Dispersion of ventricular repolarization and refractory period. Cardiovasc Res 2001;50:10–23.

[2] Li GR, Feng J, Yue L, Carrier M. Transmural heterogeneity of action potentials and I_{to1} in myocytes isolated from the human right ventricle. Am J Physiol 1998;275:H369–H377.

[3] Wettwer E, Amos GJ, Posival H, Ravens U. Transient outward current in human ventricular myocytes of subepicardial and subendocardial origin. Circ Res 1994;75:473–482.

[4] Näbauer M, Beuckelmann DJ, Überfuhr P, Steinbeck G. Regional differences in current density and rate-dependent properties of the transient outward current in subepicardial and subendocardial myocytes of human left ventricle. Circ 1996;93:168–177.

[5] Zicha S, Xiao L, Stafford S, Cha TJ, Han W, Varro A, Nattel S. Transmural expression of transient outward potassium current subunits in normal and failing canine and human hearts. J Physiol 2004;561.3:735–748.

[6] Liu DW, Antzelevitch C. Characteristics of the delayed rectifier current (I_{Kr} and I_{Ks}) in canine ventricular epicardial, midmyocardial and endocardial myocytes: a weaker I_{Ks} contributes to the longer action potential of the M cell. Circ Res 1995;76:351–365.

[7] Zygmunt AC, Goodrow RJ, Antzelevitch C. I(NaCa) contributes to electrical heterogeneity within the canine ventricle. Am J Physiol 2000;278:H1671–H1678.

[8] Volders PGA, Sipido KR, Carmeliet E, Spätjens RLHMG, Wellens HJJ, Vos MA. Repolarizing K+ currents ITO1 and IKS are larger in right than left canine ventricular midmyocardium. Circ 1999;99:206–210.

[9] Bauer A, Becker R, Karle C, Schreiner KD, Senges JC, Voss F, Kraft P, Kuebler W, Schoels W. Effects of the I_{Kr}-blocking agent Dofetilide and of the I_{Ks}-blocking agent Chromanol 293B on regional disparity of left ventricular repolarization in the intact canine heart. J Cardiovasc Pharmacol 2002;39:460–467.

[10] ten Tusscher KHWJ, Noble D, Noble PJ, Panfilov AV. A model for human ventricular tissue. Am J Physiol 2004; 286:H1573–H1589.

[11] Visible Human Project, National Library of Medicine, Bethesda, USA.

[12] Ramanathan C, Jia P, Ghanem R, Ryu K, Rudy Y. Activation and repolarization of the normal human heart under complete physiological conditions. PNAS 2006; 103(16):6309–6314.

[13] Janse MJ, Sosunov EA, Coronel R, Opthof T, Anyukhovsky EP, de Bakker JM, Plotnikov AN, Shlapakova IN, Danilo Peter J, Tijssen JG, Rosen MR. Repolarization Gradients in the Canine Left Ventricle Before and After Induction of Short-Term Cardiac Memory. Circulation 2005; 112(12):1711–1718.

[14] van Oosterom A. Genesis of the T wave as based on an equivalent surface source model. J Electrocardiol 2001; 34(Suppl):217–27.

Address for correspondence:

Dipl.-Ing. Daniel L. Weiss
Institute of Biomedical Engineering, Universität Karlsruhe (TH)
Kaiserstr. 12, 76128 Karlsruhe, Germany
tel./fax. ++49 721 608 2790/2789
Daniel.Weiss@ibt.uni-karlsruhe.de